A Methodology to Evaluate the Effects of Kinematic Measurement Uncertainties on Knee Ligament Properties Estimated from Laxity Measurements

Andersen, Michael Skipper; Dzialo, Christine Mary; Marra, Marco Antonio; Pedersen, Dennis

Published in:
Journal of Biomechanical Engineering

DOI (link to publication from Publisher):
10.1115/1.4050027

Publication date:
2021

Document Version
Accepted author manuscript, peer reviewed version

Citation for published version (APA):
Andersen, M. S., Dzialo, C. M., Marra, M. A., & Pedersen, D. (2021). A Methodology to Evaluate the Effects of Kinematic Measurement Uncertainties on Knee Ligament Properties Estimated from Laxity Measurements. *Journal of Biomechanical Engineering*, *143*(6), Article 061003. https://doi.org/10.1115/1.4050027

A methodology to evaluate the effects of kinematic measurement uncertainties on knee ligament properties estimated from laxity measurements

Andersen, Michael Skipper[1]
Department of Materials and Production
Aalborg University
Fibigerstraede 16, DK-9220 Aalborg East
msa@mp.aau.dk

Dzialo, Christine Mary
Department of Materials and Production
Aalborg University
Fibigerstraede 16, DK-9220 Aalborg East
christinedzialo@gmail.com

Marra, Marco Antonio
University of Twente
Faculty of Engineering Technology
Horst Complex W104
P.O. Box 217
7500 AE Enschede
The Netherlands
m.a.marra@utwente.nl

Pedersen, Dennis
Regional Development
Central Denmark Region
Skottenborg 26
8800 Viborg
Denmark
dennis.pedersen@ru.rm.dk

[1] Corresponding author.

A methodology to evaluate the effects of kinematic measurement uncertainties on knee ligament properties estimated from laxity measurements

ABSTRACT

Ligaments are important joint stabilizers but assessing their mechanical properties remain challenging. We developed a methodology to investigate the effects of kinematic measurement uncertainty during laxity tests on optimization-based estimation of ligament properties. We applied this methodology to a subject-specific knee model with known ligament properties as inputs and compared the estimated to the known knee ligament properties under the influence of noise. Four different sets of laxity tests were simulated with an increasing number of load cases, capturing anterior/posterior, varus/valgus and internal/external rotation loads at 0° and 30° of knee flexion. 20 samples of uniform random noise ([-0.5,0.5] mm and degrees) were added to each set and fed into an optimization routine that subsequently estimated the ligament properties based on the noise targets. We found a large range of estimated ligament properties (stiffness ranges of 5.97kN, 7.64kN, 8.72kN, and 3.86kN; reference strain ranges of 3.11%, 2.53%, 1.88% and 1.58% for ACL, PCL, MCL, and LCL, respectively) for three sets of laxity tests, including up to 22 load cases. A set of laxity tests with 60 load cases kept the stiffness and reference strain ranges below 470N per unit strain and 0.85%, respectively. These results illustrate that kinematic measurement noise have a large impact on estimated ligament properties and we recommend that future studies assess and report both the estimated ligament properties and the associated uncertainties due to kinematic measurement noise.

INTRODUCTION

Joint stability plays a vital role for the function of the knee and the presence of instability can cause pain, joint degradation, decreased mobility, and an overall reduced quality-of-life [1,2]. Given its non-conforming nature, the stability of the knee is primarily maintained by the ligaments and muscles in addition to the condyle shapes and menisci [3]. However, the contribution of ligaments to joint stability has been investigated mostly using *in vitro* methods [4], as these tissues are typically very difficult to assess *in vivo*.

Due to their ability to estimate muscle, ligament, and joint contact forces, patient-specific computational knee models have the potential to aid in better understanding of healthy and pathological knee mechanics. Additionally, these models can potentially be applied to pre-operative surgical planning with the aim of supporting the surgeon in selecting the treatment that best restores the joint mechanics. This is specifically relevant for joint replacements, where surgical techniques, implant size, position, and component geometry affect the post-operative joint stability and joint mechanics that can subsequently affect the short- and long-term outcome [5].

To create a computational knee model, either a finite element [6-8] or rigid-body [7,9] modeling approach can be taken. These methods require geometry, typically derived from medical images, and models of the cartilage, meniscus, ligaments, and other stabilizing structures, such as the posterior capsule. The elastic structures are described through nonlinear constitutive equations that require the identification of tissue-specific parameters. These are typically acquired from mechanical testing of cadaveric tissues, e.g. for cartilage [10] and ligaments [11]. However, this approach has two major drawbacks: 1) the parameters are not necessarily representing the properties of a given subject and 2) some properties, such as the ligament pre-tension, cannot be measured on the cadaveric tissue. Therefore, recent approaches have applied optimization techniques to estimate subject-specific ligament properties from laxity measurements [8,12]. Naghibi Beidokhti et al. [8] applied five levels of internal-external rotational moment and four levels of varus/valgus moment at 0°, 30°, 60°, and 90° tibiofemoral flexion on three cadaveric knees and measured the resulting position and orientation of tibia, femur, and patella using an electromagnetic tracking system. These measurements were applied to estimate the ligament properties of both spring and continuum mechanics models. Ewing et al. [12] applied a knee laxity testing device, developed for intraoperative laxity assessments, to measure and optimize the ligament properties of cadaver-specific knee models following total knee arthroplasty. To this end, they used measurements of the varus/valgus angle at both full extension and 90° tibiofemoral flexion under ± 20 Nm varus/valgus moment, the internal/external rotation angle at approximately ± 10 Nm internal/external moment at full extension, and the knee flexion/extension angle under no load to optimize 18 ligament parameters. These studies both demonstrated that estimated ligament properties vary between subjects and that model predictions improve with optimized ligament properties. However, these studies used navigation systems to measure the joint kinematics, which are feasible in cadavers or intraoperatively, but not for assessments in healthy subjects or pre-operative planning; highlighting the necessity of non-invasive methodologies. Therefore, we have recently developed a technology to measure 4-DOF laxity non-invasively by combining a loading device and EOS biplanar x-rays [13]. However, independent of whether a navigation system or x-rays are used to estimate knee kinematics, these are affected by measurement errors. The specific errors depend on a series of factors including, but not limited to, the manufacturer, sampling rate, sensor positions, calibrations etc. A recent study of one the leading marker-based systems, Vicon (Vicon Motion Systems Ltd, Oxford, United Kingdom), showed static measurement errors on a single marker of 0.15 mm and 0.35 mm during slow dynamic (< 1 m/s) situations under optimized marker size and sampling frequency conditions; while errors up to 2 mm were also observed [14]. In terms of reconstructions based on EOS bi-planar x-rays, Pedersen et al. [13] found Root-Mean-Square (RMS) errors of 0.88 mm and 0.49° for tibiofemoral translations and rotations when comparing bone pose estimations based on bone contours and a bone fixed marker frame. Given the relatively high stiffness reported for ligaments, it remains unknown how these kinematic measurement errors affect the identified ligament properties and furthermore, how these errors interacts with the number and type of laxity measurements included in the identification process.

Therefore, the aim of this study was to development a methodology to quantify the effects of kinematic measurement errors on the estimation of knee ligament properties. This methodology we applied to investigate how kinematic measurement noise during laxity measurements affect the estimation of ligament properties. To this end, we developed a knee model with known ligament properties, we then performed a series of laxity tests on this model and to the resulting pose between femur and tibia, we added random noise to simulate kinematic measurement noise. The noisy target data were subsequently used to identify the ligament properties using optimization. Finally, the estimated ligament properties were then compared to the known ligament properties that were input to the model in the first place. An overview of the study is depicted in Fig. 1.

METHODS

Experimental data

Medical Resonance Imaging (MRI) scans were obtained of the right knee of a female subject (27-year-old, 1.72 m, 61.2 kg) using a 1.5 T General Electric Discovery scanner and a quad knee coil. The acquisitions taken (SAG FSPGR 3D FS, slice thickness = 1 mm, resolution 512 square pixels, 160 mm reconstruction diameter (Field-of-view (FOV)), 100 images in acquisition and COR SPGR 3D, slice thickness = 1 mm, space between slices 0.5mm, resolution 512 square pixels, 160 mm reconstruction diameter (FOV), 192 images in acquisition) were based on the Osteoarthritis Initiative (OAI) protocol [15] and adapted to a General Electric scanner [16]. These scans were selected to clearly distinguish between bone, articular cartilage, menisci, and ligament attachment regions. We refer to this scan as the *Detailed knee* scan. Additionally, the lower extremities were imaged using a 3T Siemens Prisma MRI (COR T1W-Vibe-Dixon, slice thickness = 1.4 mm, space between slices 0.0 mm, resolution 320 square pixels, FOV 440 mm x 440 mm, (160 pelvis, 140 knee, 192 ankle) images in acquisitions) and a Peripheral Angio 36 coil. To cover the full lower limbs, three acquisitions were taken and subsequently stitched together by the radiologist using custom Siemens software and exported as Digital Imaging and Communications in Medicine (DICOM) files. We refer to this series of images as the *Lower Limbs* scan. The study was conducted in accordance with the ethical guidelines of The Scientific Ethical Committee for the Region of North Jutland (Den Videnskabsetiske Komité for Region Nordjylland).

Tibiofemoral Joint Model

The tibiofemoral joint model was created in the AnyBody Modeling System v. 7.1 (AnyBody Technology A/S, Aalborg, Denmark). The required anatomical structures (bones, articular cartilages, and ligaments) were segmented from the *Detailed knee* scans using Mimics Research v. 18.0 (Materialise, Leuven, Belgium) and saved as stereolithographyfiles. Additionally, the ligament origin and insertion sites, as well as bony landmarks for definition of anatomical coordinate systems, were identified on the segmentations. To identify the hip and ankle joint centers, the femur and tibia were segmented from the *Lower Limbs* scan and registered to the bone segmentations in the *Detailed knee scan*. The hip center was identified by performing a spherical fit to the femoral head and the ankle joint center found as the midpoint between two spheres fitted to the articulating surface of talus as described by Parra et al. [17]. The knee center and flexion axis were identified by cylinder fits to the medial and lateral femoral articular surfaces following the procedure described by Dzialo et al. [18] to determine the extension facet centers. In addition to the hip and ankle joint centers, the medial and lateral femoral epicondyles and the medial and lateral tibial plateau edges were manually selected and applied to define anatomical coordinate systems for femur and tibia following the ISB recommendations [19].

The model only included the femur and tibia bones (with articular cartilages) and respective ligaments. The femur was fixed relative to the global coordinate system such that the anatomical coordinate system of femur aligned with the global axis, and the knee flexion angle specified to either 0° or 30° (see below) depending on the specific laxity trial being simulated. A reaction moment was included around the knee flexion axis to simulate a fixated knee angle. The remaining five Degrees-Of-Freedom (DOF) of the tibiofemoral joint were modeled using the Force-Dependent Kinematics (FDK) methodology [20,21], enabling computation of the movements in these DOFs based on static equilibrium between the contact, ligament, and external forces and moments. An elastic foundation contact model with a pressure modulus of 10 GNm^{-3} was applied to model the contact between the femoral and tibial (medial and lateral) articular cartilages. A tolerance of 0.001 N (Nm for moments) was applied when solving for the static equilibrium.

The Anterior and Posterior Cruciate Ligaments (ACL and PCL) and the Medial and Lateral Collateral Ligaments (MCL and LCL) were defined by one line element each with a nonlinear force-strain relationship, consisting of a slack region, a polynomial toe region at low strain and a linear region for high strain [22]:

$$f(\varepsilon) = \begin{cases} \frac{k\varepsilon^2}{4\varepsilon_l}, & 0 \leq \varepsilon \leq 2\varepsilon_l \\ k(\varepsilon - \varepsilon_l), & \varepsilon \geq 2\varepsilon_l \\ 0, & \varepsilon \leq 0 \end{cases} \quad (1)$$

where $f(\varepsilon)$ is the tensile force in the ligament, k is the stiffness, ε is the instantaneous strain, and ε_l is the linear strain limit, which was set to 0.03 [11]. The slack length, l_0, was computed based on the defined origin and insertion locations in the *Detailed knee* scan such that:

$$l_0 = \frac{l_r}{\varepsilon_r + 1} \quad (2)$$

where l_r is the ligament length in the *Detailed knee* scan and ε_r is the reference strain. Finally, the instantaneous strain, ε, during the simulation was computed from the instantaneous ligament length, l , as follows:

$$\varepsilon = \frac{l - l_0}{l_0} \qquad (3)$$

The applied ligament properties are shown in Table 1 and derived based on ligament properties reported in the literature [21,23].

Baseline Laxity Trials and Noise

Four different sets of laxity tests (depicted in Table 2) were performed on the model and we refer to these as Set 1, Set 2, Set 3 and Set 4. All loads were defined to align with the global coordinate system, and coincidently to the femoral anatomical coordinate system, and therefore remained fixed when tibia translated or rotated under load. Forces were applied to the tibial tuberosity; while varus/valgus and internal/external rotation loads were applied as pure moments on the tibia. All sets contained anterior, posterior, varus, valgus, internal, and external load directions at either 0° or 30° of knee flexion. The load cases for each set were constructed to have an increasing number of load magnitudes and knee flexion angles for each load direction, as this was expected to improve the estimation of the ligament properties in the presence of measurement noise. The laxity tests with known ligament properties were used as the baseline translations and rotations under each load case; from which 20 simulated laxity measurement tests for each set were created by randomly adding uniform noise in the intervals [-0.5 mm, 0.5 mm] and [-0.5°, 0.5°] for translations and rotations, respectively. This setup replicates the situation where the laxity tests are repeated 20 times but each time the measurement noise is different.

Optimization of Ligament Properties

For each of the noisy target data (20 in each of set), we set up an optimization problem to identify the ligament properties resulting in the best match between model-predicted translations and rotations, and the noisy target data. To this end, the following least-squares optimization problem was set up:

$$\begin{aligned} &\min_{d} \Psi^T \Psi \\ s.t. \quad &F_j^{(\mathrm{FDK})} < \varepsilon^{(\mathrm{FDK})} \\ &k_i \geq 0, \quad i = 1, \dots 4 \end{aligned} \tag{4}$$

Where d is a vector containing the ligament stiffness values, k_i, and the reference strains to be identified, and i is refering to the ith ligament. Ψ is a vector of differences between the model-predicted translations and rotations and the noisy target translations and rotations. $F_j^{(\mathrm{FDK})}$ is the maximum FDK residual force and moment for the jth laxity trial and $\varepsilon^{(\mathrm{FDK})}$=0.001 is the tolerance on the static equilibrium.

Due to the potential of introducing knee instability by varying the ligament properties and the numerical difficulties in solving the FDK contact problem, we decided to apply the zeroth-order Complex optimization method [24]. Although the method is computationally more expensive than gradient-based optimizers, we chose it due to its robustness and because it does not require gradient information. The Complex optimizer was developed for unconstrained optimization problems and in order to apply it to Equation (4), we handled the inequality constraints through penalization. If any of the FDK residual forces or moments were above the tolerance or any of stiffness values below zero, then these values were squared, multiplied by a penalty factor of 100, and added to the objective function.

Within the Complex optimizer, a population of design variables was initially created and randomly distributed over the design domain. These we randomly scattered around the known ligament properties (Table 2) such that the optimizer would find these as the optimum, if they indeed were the optimum of the problem. Hereby, the risk of finding a nearby local minimizer was reduced. Stiffness values and reference strains were uniformly sampled in the intervals of ±500 N and ±0.02 of the known value, respectively. Finally, we applied a population size of 17, which is significantly larger than the number of design variables (eight).

To converge towards the optimum, for each iteration, the Complex method identifies the poorest element in the population and improves it by projecting this element across the centroid of the other elements, leading to a steady improvement and convergence towards a local minimizer. To improve robustness of the algorithm, if the projected element remains the poorest, the next projection is steered towards the best element. Should it still remain the poorest after four attempts, the element is replaced by a new random element and the algorithm reset. The Complex algorithm and optimization problem were implemented in Matlab R2015b (Mathworks, Massachusetts, USA) using custom code that executed the AnyBody model for every change in the design variables.

RESULTS

The forces in each ligament under all load cases of Set 3 are illustrated in Fig. 2. As seen in the figure, all ligaments show a variation in the forces between the load cases. For all ligaments except PCL, it is also clear that it is possible to identify a load case, where the specific ligament is loaded relatively more than other ligaments, i.e. the anterior load case at 0° for ACL, varus loading at 30° for LCL, and valgus loading at 0° for MCL. PCL, however, not only show the lowest forces but also seem to be recruited together with one or more other ligaments when it is recruited.

The estimated ligament properties from the noisy data are depicted as boxplots in Fig. 3. Additionally, the minimum and maximum stiffness values and reference strains were identified from the 20 noisy laxity trials of each set of laxity tests and recorded in Table 3. Overall, by a large margin, Set 4 produced the closest match to the true ligament properties with a range of estimated for stiffness values and reference strains of at most 400 N per unit strain and 0.39 %, respectively. Among the other three sets, there was not a clear difference in the ability to mitigate the kinematic measurement noise, with Set 1 producing the largest error of 7.31 kN for MCL, Set 2 the largest error of 2.34 kN for LCL, and Set 3 the largest errors of 3.49 kN and 4.32 kN for ACL and PCL, respectively. For the reference strains, Set 1 produced the largest errors of 1.93 % for ACL and 1.75 % for PCL; while Set 2 produced the largest errors of 2.44 % and 1.00 % for MCL and LCL, respectively.

For the sets with the fewest number of load cases (Sets 1 to 3), we found a large range of estimated ligament properties with ACL stiffness varying by 5.97 kN, PCL by 7.64 kN, MCL by 8.72 kN, and LCL by 3.86 kN. The identified reference strains also varied substantially with ACL varying by up to 3.11%, PCL by 2.53%, MCL by 1.88%, and LCL by 1.58%. On the contrary, Set 4, containing 60 different load cases, resulted in stiffness values and reference strains that matched much closer the true ligament properties in the presence of noise with ranges of at most 470 N and 0.85% for stiffness and reference strain, respectively.

DISCUSSION

The purpose of this study develop a methodology to estimate the effects of kinematic measurement noise during laxity tests on estimated ligament properties. We applied this method on a simple knee model, containing the ACL, PCL, MCL, and LCL, each modeled as a single line element with ligament properties based on literature values. This model was subjected to four different sets of simulated laxity tests with an increasing number of load cases in each. Uniform random noise was then added to the resulting knee translations and rotations to simulate measurements with errors on the same order of magnitude as can be expected when these measurements are performed in practice [13,14]. However, we opted to not include the extreme errors reported, as the probability of these occurring is not known and instead focused on a smaller interval where the measurements are expected to be all the time. Based on the noisy target data, we applied an optimization method to estimate the ligament properties that resulted in the smallest least-square difference between the noisy target data and the model predictions.

Our results showed a large range of estimated ligament properties for the three sets of laxity tests with the fewest number of load cases (1-3) (ACL stiffness varying by 5.97 kN, PCL by 7.64 kN, MCL by 8.72 kN, and LCL by 3.86 kN. Reference strains also varied substantially with ACL varying by up to 3.11%, PCL by 2.53%, MCL by 1.88%, and LCL by 1.58%). Only, Set 4, containing 60 different load cases, resulted in stiffness values and reference strains that matched much closer the true ligament properties in the presence of noise with the largest range of estimated stiffness of 470 N and range of reference strain 0.85%.

To identify ligament properties, recent studies [8,12] have applied measurements of subject-specific laxity and run optimization methods to identify the ligament properties that resulted in the smallest difference between the measurements and predictions by a knee model utilizing the properties. While this currently seems like the only viable approach to identify both stiffness values and reference strains, the results of our study show that the level of kinematic measurement noise currently associated with the measurement of tibiofemoral kinematics during laxity tests can have a large influence on the identified properties. In an optimization problem with only eight variables (two for each of the four ligaments), only Set 4 of laxity trials with 60 different load cases was able to keep the effect of the kinematic measurement noise relatively small. Merely including 22 load cases, i.e. almost three times more measurements than unknown parameters, was insufficient to mitigate the effect of the noise.

At this point, there is no consensus in the literature about 1) how the knee ligaments are best modeled and 2) which laxity measurements are best suited to identify these parameters. For this reason, we cannot infer from our results how other setups are affected by measurement noise. However, we do anticipate that if each ligament in our model were represented by multiple elements that the effect of the measurement noise would be amplified and that it would take a larger number of laxity measurements to mitigate the error. As developed methodology presented here can easily be replicated in other models and measurement inputs, we recommend that future studies provide an indication of the uncertainty on the identified ligament properties.

It is important to stress that we did not attempt to identify the laxity tests that were best at attenuating the measurement noise. Other combinations of well-known laxity tests that perform better may, therefore, exist. For instance, inclusion of laxity tests at higher knee flexion angles could have been included, e.g. at 60° or 90°, that are also used clinically. The main reason for not including high knee flexion angles were due to possible instability issues with the simplified knee model. As the ligaments were only represented by one bundle each, when the knee is highly flexion, both the MCL and LCL have a tendency to become slack, leaving only two ligament bundles to balance the external loads. From an isolation perspective, this is good, but while the static equilibrium may still exist, finding it for the numerical solver becomes challenging.

Hence, to enable inclusion of laxity tests at high knee flexion angles, the model should be extended to include more ligament bundles. This of course has the drawback that more laxity tests most likely must be included to be able to identify the mechanical properties of each bundle. Therefore, future research should investigate which set of laxity tests are best suited to attenuate the effects of measurement uncertainties. To fully clarify this, more sophisticated knee models should be applied as well. With that being said, from the load cases included for Set 3 (see Fig. 2), the variations in force of ACL, MCL and LCL indicate that, at least in this set, sufficient load cases are included. PCL does also show variations in force between the different load cases, but always vary with one or more other ligaments. However, these observed variations indicate that, at least for Set 3, the errors in the estimated ligament properties is associated primarily with the kinematic measurement noise and not a lack of load cases to resolve the redundancy problem associated with estimating the ligament properties in the absence of noise.

Our study includes several important limitations. First of all, we only studied one specimen. Bone geometry and ligament attachments have inter-individual variations and may, therefore, respond slightly differently to applied external loads. Therefore, we anticipate that measurement noise during laxity measurements will migrate slightly differently to each ligament for each subject. Secondly, we modeled each ligament as a single spring. If more bundles were to be included, we anticipate that more load cases would be required to mitigate the measurement noise, but this should be evaluated in future studies. Third, due to the computational cost of repeatedly running these optimizations, we only included 20 random samples for each of the four sets of laxity tests. As we assumed the noise to be uniformly distributed around the true value, we expect that the average error will converge to zero as the number of samples increases and thus, the average is not of interest in this study. However, the range of the identified ligament properties is of interest as it indicates the interval that an identified ligament property is within. With only 20 samples, we expect that this range is under-predicted but for the first three sets tested (1-3), we have already found a large range of ligament properties, showing that measurement noise has an important impact. If the measurement errors are uniformly or normally distributed, a potential solution approach is to repeat the laxity measurements multiple times and determine the average properties that are likely to have the lowest error. Fourth, we assumed noise magnitudes of 0.5 mm and 0.5°; however, this may not be representative of all measurement systems. As the specific noise magnitude and distribution is system-dependent, we cannot generalize the results. However, the noise we have included is on the low end of what has been reported for some systems. [13,14]. Pedersen et al. [13] found RMS errors of 0.88 mm and 0.49° for tibiofemoral translations and rotations but average limits of agreements between bone pin reconstructions and contour reconstructions between −1.64 mm and 1.80 mm for translations and −0.85° and 1.05° for rotations. Hence, with this system, the error ranges on ligament properties reported in the current paper are likely under-estimated as compared to if those inputs were used. Merriaux et al. [14] found errors of 0.35 mm of a single marker using Vicon markers under slow dynamic conditions with optimized conditions. How this error translates to joint kinematic errors depend on bone pin marker positions etc., but will likely result in errors larger than 0.35 mm for translations. Hence, our results may be relatively close to what can be expected with bone pin marker measurements. Last but not least, we did not include the meniscus in the model. While it does affect knee stability, its properties are rarely part of the identification process when estimating ligament properties. We could have included a meniscus in the model but since we do not know the error range in properties typically applied, we opted to leave it out and focused instead on the largest contributors to joint stability, namely the ligaments. Our presented methodology does allow inclusion of more structures in future studies.

In conclusion, we investigated the effect of measurement errors during laxity tests on optimization-based identified ligament properties and found that sub-millimeter and sub-degree errors can result in estimation errors of several thousand Newton per unit strain in stiffness and several percent in reference strain. Therefore, in addition to improving the accuracy of the measurement systems, future studies should aim to identify a set of laxity tests that results in the best robustness to noise, and identified ligament properties should be accompanied with estimated error margins.

FUNDING

A methodology to evaluate the effects of kinematic measurement uncertainties on knee ligament properties estimated from laxity measurements

This work was supported by the Sapere Aude program of the Danish Council for Independent Research (DFF) under grant number DFF-4184-00018, the Innovation Fund Denmark under the Individualized Osteoarthritis Interventions project and by the European Research Council under the European Union's Seventh Framework Programme (FP/2007–2013), ERC Grant Agreement no. 323091.

A methodology to evaluate the effects of kinematic measurement uncertainties on knee ligament properties estimated from laxity measurements

NOMENCLATURE

ACL	anterior cruciate ligament
DICOM	digital imaging and communications in medicine
DOF	degrees-of-freedom
$F_j^{(\mathrm{FDK})}$	the maximum fdk residual force and moment for the *j*th laxity trial
FDK	force-dependent kinematics
FOV	field-of-view
LCL	lateral collateral ligament
MCL	medical collateral ligament
MRI	medical resonance imaging
OAI	osteoarthritis initiative
PCL	posterior cruciate ligament
RMS	root-mean-square
d	vector of design variables
f	tensile force in a ligament
k	ligament stiffness
k_i	the stiffness of the *i*th ligament
l	instantaneous ligament length

l_0	ligament slack length
l_r	ligament reference length
ε	instantaneous ligament strain
$\varepsilon^{(\mathrm{FDK})}$	tolerance applied when solving the static equilibrium
ε_l	ligament linear strain limit
Ψ	vector of differences between model-predicted translations and rotations and noise measurement targets

REFERENCES

[1] Wheaton M, Jensen N. The ligament injury connection to osteoarthritis. Journal of Prolotherapy 2010;2:294-304.

[2] Nevitt MC, Tolstykh I, Shakoor N, Nguyen UD, Segal NA, Lewis C et al. Symptoms of knee instability as risk factors for recurrent falls. Arthritis care & research 2016;68:1089-97.

[3] Woo SL, Debski RE, Withrow JD, Janaushek MA. Biomechanics of knee ligaments. Am J Sports Med 1999;27:533-43.

[4] Athwal KK, Hunt NC, Davies AJ, Deehan DJ, Amis AA. Clinical biomechanics of instability related to total knee arthroplasty. Clin Biomech 2014;29:119-28.

[5] Victor J. Optimising position and stability in total knee arthroplasty. EFORT open reviews 2017;2:215-20.

[6] Erdemir A. Open Knee: Open Source Modeling and Simulation in Knee Biomechanics. J Knee Surg 2016;29:107-116.

[7] Halonen KS, Dzialo CM, Mannisi M, Venäläinen MS, de Zee M, Andersen MS. Workflow assessing the effect of gait alterations on stresses in the medial tibial cartilage - combined musculoskeletal modelling and finite element analysis. Sci Rep 2017;7:17396.

[8] Naghibi Beidokhti H, Janssen D, van de Groes S, Hazrati J, Van den Boogaard T, Verdonschot N. The influence of ligament modelling strategies on the predictive capability of finite element models of the human knee joint. J Biomech 2017;65:1-11.

[9] Lenhart RL, Kaiser J, Smith CR, Thelen DG. Prediction and Validation of Load-Dependent Behavior of the Tibiofemoral and Patellofemoral Joints During Movement. Ann Biomed Eng 2015;43:2675-85.

[10] Korhonen RK, Laasanen MS, Töyräs J, Rieppo J, Hirvonen J, Helminen HJ et al. Comparison of the equilibrium response of articular cartilage in unconfined compression, confined compression and indentation. J Biomech 2002;35:903-9.

[11] Butler DL, Kay MD, Stouffer DC. Comparison of material properties in fascicle-bone units from human patellar tendon and knee ligaments. J Biomech 1986;19:425-32.

[12] Ewing JA, Kaufman MK, Hutter EE, Granger JF, Beal MD, Piazza SJ et al. Estimating patient-specific soft-tissue properties in a TKA knee. J Orthop Res 2016;34:435-443.

[13] Pedersen D, Vanheule V, Wirix-Speetjens R, Taylan O, Delport H, Scheys L et al. A novel non-invasive method for measuring knee joint laxity in four dof: In vitro proof-of-concept and validation. Journal of Biomechanics 2018.

[14] Merriaux P, Dupuis Y, Boutteau R, Vasseur P, Savatier X. A Study of Vicon System Positioning Performance. Senors 2017;17(7):1591.

[15] Peterfy CG, Schneider E, Nevitt M. The osteoarthritis initiative: report on the design rationale for the magnetic resonance imaging protocol for the knee. Osteoarthritis and Cartilage 2008;16:1433-41.

[16] Balamoody S, Williams TG, Waterton JC, Bowes M, Hodgson R, Taylor CJ et al. Comparison of 3T MR scanners in regional cartilage-thickness analysis in osteoarthritis: a cross-sectional multicenter, multivendor study. Arthritis Research & Therapy 2010;12:R202.

[17] Parra WCH, Chatterjee HJ, Soligo C. Calculating the axes of rotation for the subtalar and talocrural joints using 3D bone reconstructions. J Biomech 2012;45:1103-7.

[18] Dzialo CM, Pedersen PH, Simonsen CW, Jensen KK, de Zee M, Andersen MS. Development and validation of a subject-specific moving-axis tibiofemoral joint model using MRI and EOS imaging during a quasi-static lunge. Journal of Biomechanics 2018;72:71-80.

[19] Grood ES, Suntay WJ. A Joint Coordinate System for the Clinical Description of Three-Dimensional Motions Application to the Knee. J Biomed Eng 1983;105:136-43.

[20] Andersen MS, de Zee M, Damsgaard M, Nolte D, Rasmussen J. Introduction to force-dependent kinematics: theory and application to mandible modeling. J Biomech Eng 2017;139:091001.

[21] Marra MA, Vanheule V, Fluit R, Koopman BHFJM, Rasmussen J, Verdonschot N et al. A Subject-Specific Musculoskeletal Modeling Framework to Predict In Vivo Mechanics of Total Knee Arthroplasty. J Biomech Eng 2015;137:020904.

[22] Blankevoort L, Huiskes R. Ligament-bone interaction in a three-dimensional model of the knee. J Biomech Eng 1991;113:263-9.

[23] Blankevoort L, Kuiper JH, Huiskes R, Grootenboer HJ. Articular contact in a three-dimensional model of the knee. J Biomech 1991;24:1019-31.

[24] Box M. A new method of constrained optimization and a comparison with other methods. The Computer Journal 1965;8:42-52.

Figure Captions List

Fig. 1 Illustration of the study workflow, starting from simulations of laxity tests with known ligament parameter inputs. Onto these, uniform random noise is added to create 20 data sets for each set of laxity tests from which the ligament parameters are estimated through optimization. The estimated parameters are finally compared to the known input parameters.

Fig. 2 Ligament forces for all load cases of Set 3.

Fig. 3 Boxplot of the estimated stiffness (top row) and reference strains (bottom row) for each of the four sets of laxity trials. The gray dots indicate the true laxity property and crosses indicate outliers among the estimated parameters.

Table Caption List

Table 1	Ligament stiffness and reference strain properties.
Table 2	Load cases for the different sets of laxity tests.
Table 3	Minimum and maximum ligament stiffness and reference strain for the four ligaments estimated from each of the four sets of laxity measurements. The table also includes the true ligament properties for easy comparison.

Fig 1.

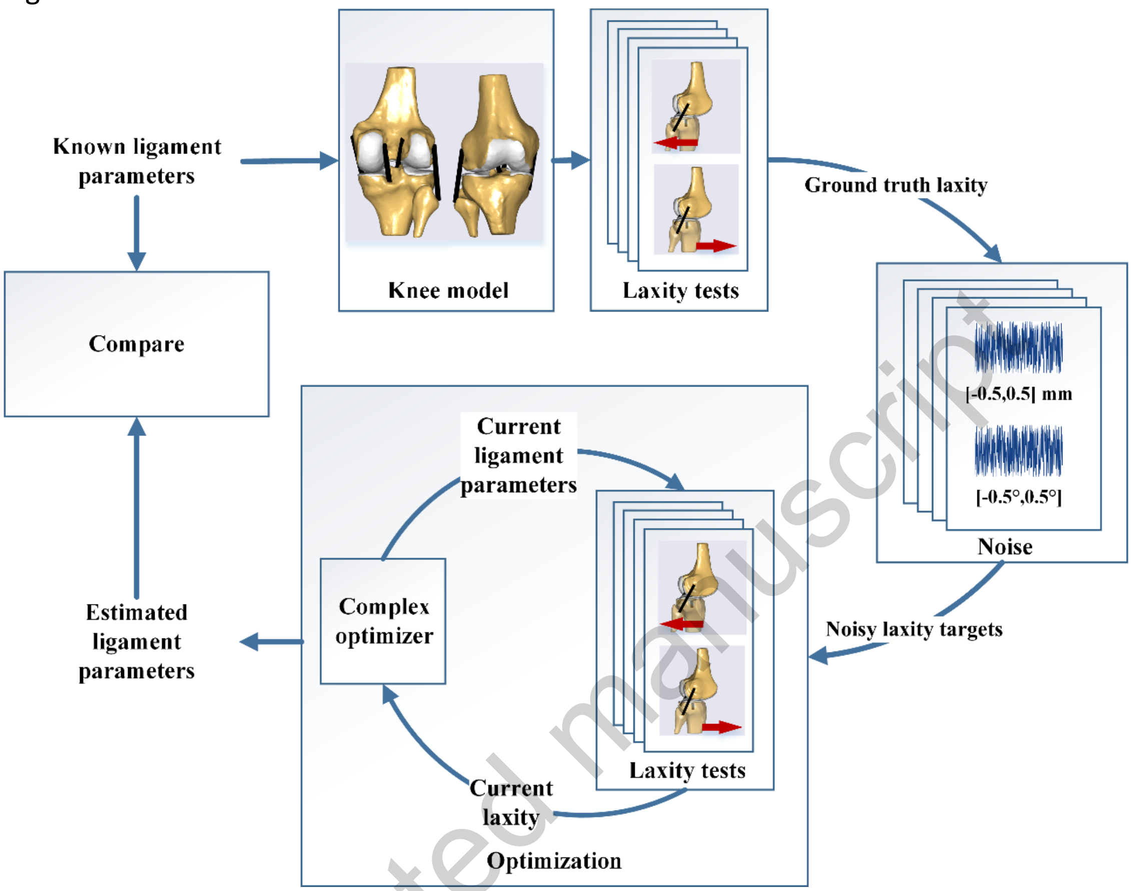
Known ligament parameters
Knee model
Laxity tests
Ground truth laxity
Compare
[-0.5,0.5] mm
[-0.5°,0.5°]
Noise
Current ligament parameters
Complex optimizer
Estimated ligament parameters
Laxity tests
Noisy laxity targets
Current laxity
Optimization

Fig 2.

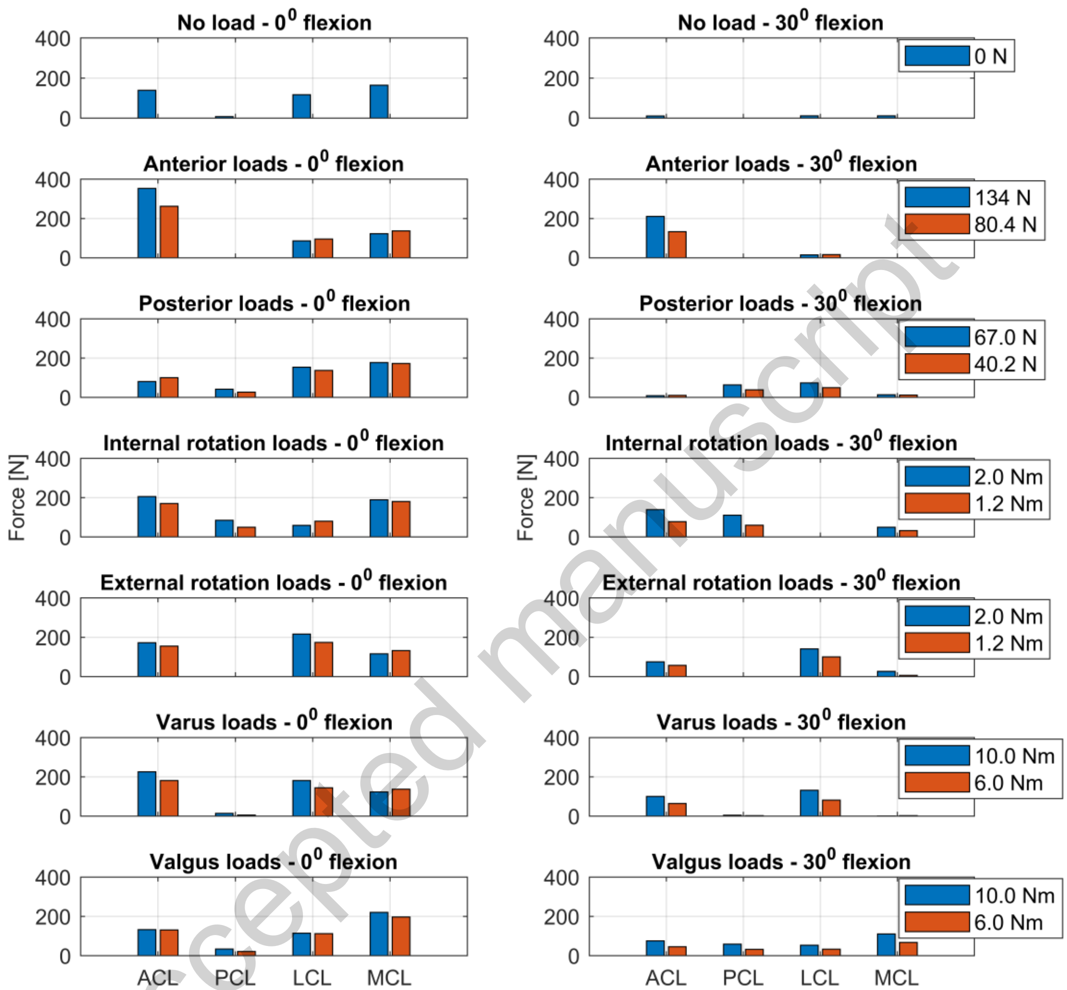

No load - 0^0 flexion
No load - 30^0 flexion
0 N
Anterior loads - 0^0 flexion
Anterior loads - 30^0 flexion
134 N
80.4 N
Posterior loads - 0^0 flexion
Posterior loads - 30^0 flexion
67.0 N
40.2 N
Internal rotation loads - 0^0 flexion
Internal rotation loads - 30^0 flexion
2.0 Nm
1.2 Nm
External rotation loads - 0^0 flexion
External rotation loads - 30^0 flexion
2.0 Nm
1.2 Nm
Varus loads - 0^0 flexion
Varus loads - 30^0 flexion
10.0 Nm
6.0 Nm
Valgus loads - 0^0 flexion
Valgus loads - 30^0 flexion
10.0 Nm
6.0 Nm
Force [N]
400
200
0
ACL
PCL
LCL
MCL

Fig 3.

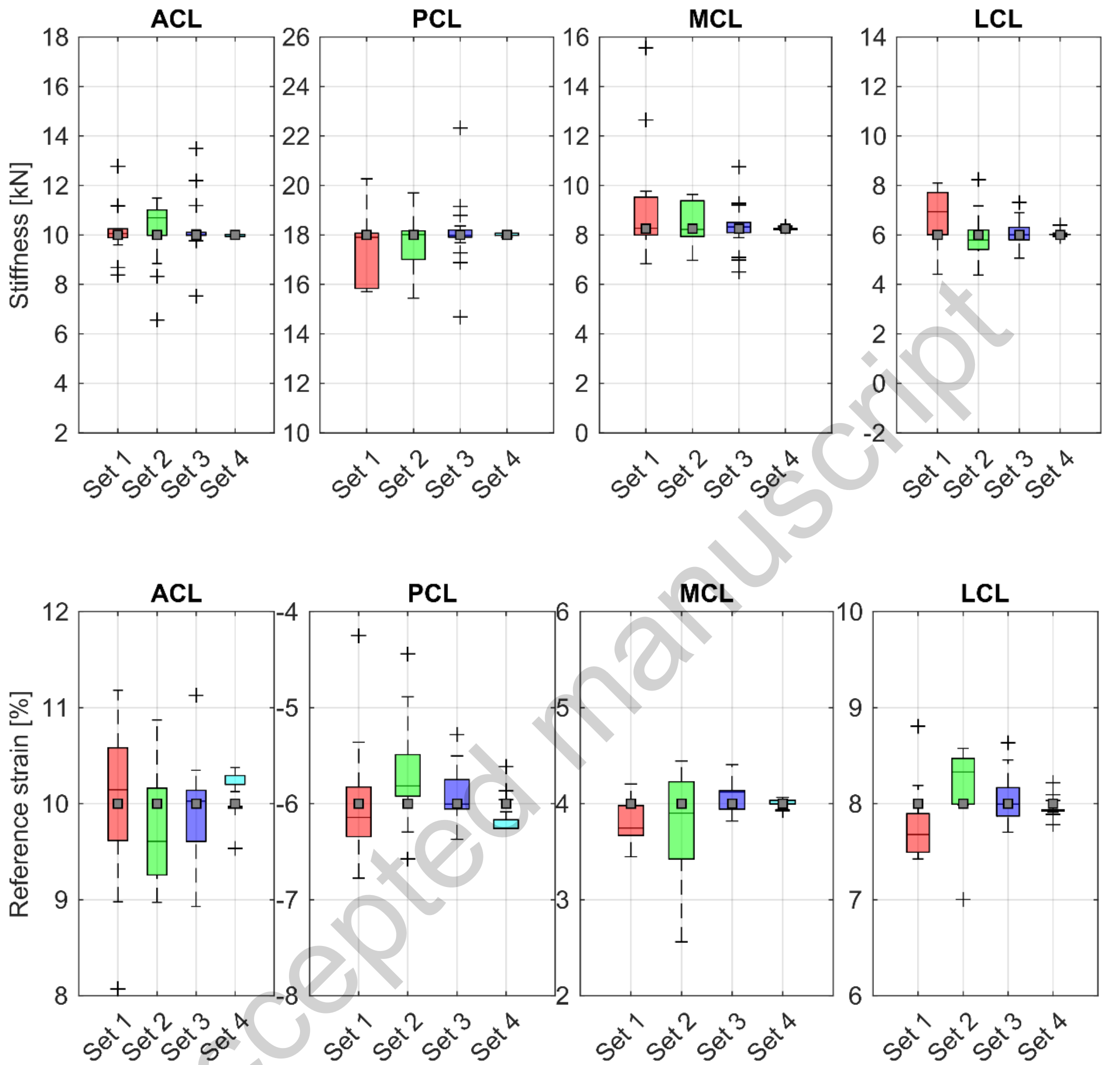
ACL
PCL
MCL
LCL
Stiffness [kN]
Reference strain [%]
Set 1
Set 2
Set 3
Set 4

Table 1.

Ligament bundle	Stiffness [kN][a]	Reference strain [%][b]
ACL	10.00	10.00
PCL	18.00	-6.00
MCL	8.25	4.00
LCL	6.00	8.00

[a]Stiffness is expressed in Newton per unit strain. [b]Reference strains are referred to the relative pose of tibia and femur in the *Detailed knee* scan.

Table 2.

Load direction	*Load magnitude*	*Knee flexion angle*
	Set 1	
No load	-	30°
Anterior	134.0 N	30°
Posterior	67.0 N	30°
Internal rotation	2.0 Nm	30°
External rotation	2.0 Nm	30°
Varus	10.0 Nm	0°
Valgus	10.0 Nm	0°
	Set 2	
No load	-	30°
Anterior	134.0, 80.4 N	30°
Posterior	67.0, 40.2 N	30°
Internal rotation	2.0, 1.2 Nm	30°
External rotation	2.0, 1.2 Nm	30°
Varus	10.0, 6.0 Nm	0°
Valgus	10.0, 6.0 Nm	0°
	Set 3	
No load	-	0°, 30°
Anterior	134.0, 80.4 N	0°, 30°
Posterior	67.0, 40.2 N	0°, 30°
Internal rotation	2.0, 1.2 Nm	0°, 30°
External rotation	2.0, 1.2 Nm	0°, 30°
Varus	10.0, 6.0 Nm	0°, 30°
Valgus	10.0, 6.0 Nm	0°, 30°
	Set 4	
No load	-	0°, 30°
Anterior	134, 107.2, 80.4, 53.6, 26.8 N	0°, 30°
Posterior	67, 53.6, 40.2, 26.8, 13.4 N	0°, 30°
Internal rotation	2.0, 1.6, 1.2, 0.8, 0.4 Nm	0°, 30°
External rotation	2.0, 1.6, 1.2, 0.8, 0.4 Nm	0°, 30°
Varus	10.0, 8.0, 6.0, 4.0, 2.0 Nm	0°, $30^{\circ *}$
Valgus	10.0, 8.0, 6.0, 4.0, 2.0 Nm	0°, 30°

*Load cases 4.0, 2.0 Nm at 30° were excluded due to numerical issues solving these with the literature-based ligament properties in Set 4.

Table 3.

Stiffness [kN]												
	ACL			PCL			MCL			LCL		
Test	True	Min	Max	True	Min	Max	True	Min	Max	True	Min	Max
Set 1	10.00	8.38	12.77	18.00	15.71	20.27	8.25	6.84	15.56	6.00	4.41	8.10
Set 2	10.00	6.56	11.49	18.00	15.44	19.70	8.25	6.97	9.64	6.00	4.38	8.24
Set 3	10.00	7.52	13.49	18.00	14.68	22.32	8.25	6.50	10.75	6.00	5.06	7.30
Set 4	10.00	9.83	10.09	18.00	17.91	18.07	8.25	8.18	8.35	6.00	5.93	6.40
Reference strain [%]												
	ACL			PCL			MCL			LCL		
Test	True	Min	Max	True	Min	Max	True	Min	Max	True	Min	Max
Set 1	10.00	8.07	11.18	-6.00	-6.78	-4.25	4.00	3.45	4.20	8.00	7.42	8.81
Set 2	10.00	8.97	10.87	-6.00	-6.58	-4.44	4.00	2.56	4.44	8.00	7.00	8.58
Set 3	10.00	8.93	11.13	-6.00	-6.37	-5.28	4.00	3.82	4.41	8.00	7.70	8.63
Set 4	10.00	9.53	10.38	-6.00	-6.26	-5.61	4.00	3.93	4.06	8.00	7.78	8.22